15086 REGOLITH BRECCIA ST. 1 216.5 g

INTRODUCTION: 15086 is a very friable regolith breccia (Fig. 1) dominated by quartz-normative mare basalt fragments and green glass fragments and spheres. It has a composition similar to local regolith compositions. It is medium-gray and subrounded, and homogeneous. A few zap pits are present on several surfaces.

15086 was collected on the east flank of Elbow Crater, about 60 m from the rim crest. It lay about 30 or 40 cm from basalt 15085 in a flat area with distinctly spaced cobbles such as 15086. It did not have a resolvable fillet despite its friability. Its orientation is known.

Figure 1. Pre-split view of 15086. S-71-47634

PETROLOGY: 15086 is a friable, porous regolith breccia whose fragment population is dominated by quartz-normative mare basalt, ranging from vitrophyric to medium-grained, and by green glass spheres and shards (Fig. 2). Wentworth and McKay (1984) determined a bulk density of 2.03 g/cm^3 (intrinsic density 3.22 g/cm^3), and calculated a porosity of 37.0%, in agreement with an SEM point-count porosity determination of 35.4%. McKay and Wentworth (1983) found it to be the most agglutinate-rich of Apollo 15 breccias (21.5% in the 20 to 500 micron fraction), even though it is immature

according to I_s/FeO (18 to 27 in McKay et al., 1984; 19 in Korotev, 1984 unpublished). They also found shock features to be minor. Nagle (1982b) reported grain size distribution, rounding, packing, and clast orientation data. Hutcheon et al. (1972) found 15086 to be the least metamorphosed breccia studied by them; it contained no shock-produced glass, indicating very low peak shock pressures, and the tracks at boundaries between small grains were not erased, indicating consolidation either by the load of overburden or a very mild, cold, shock-compaction process.

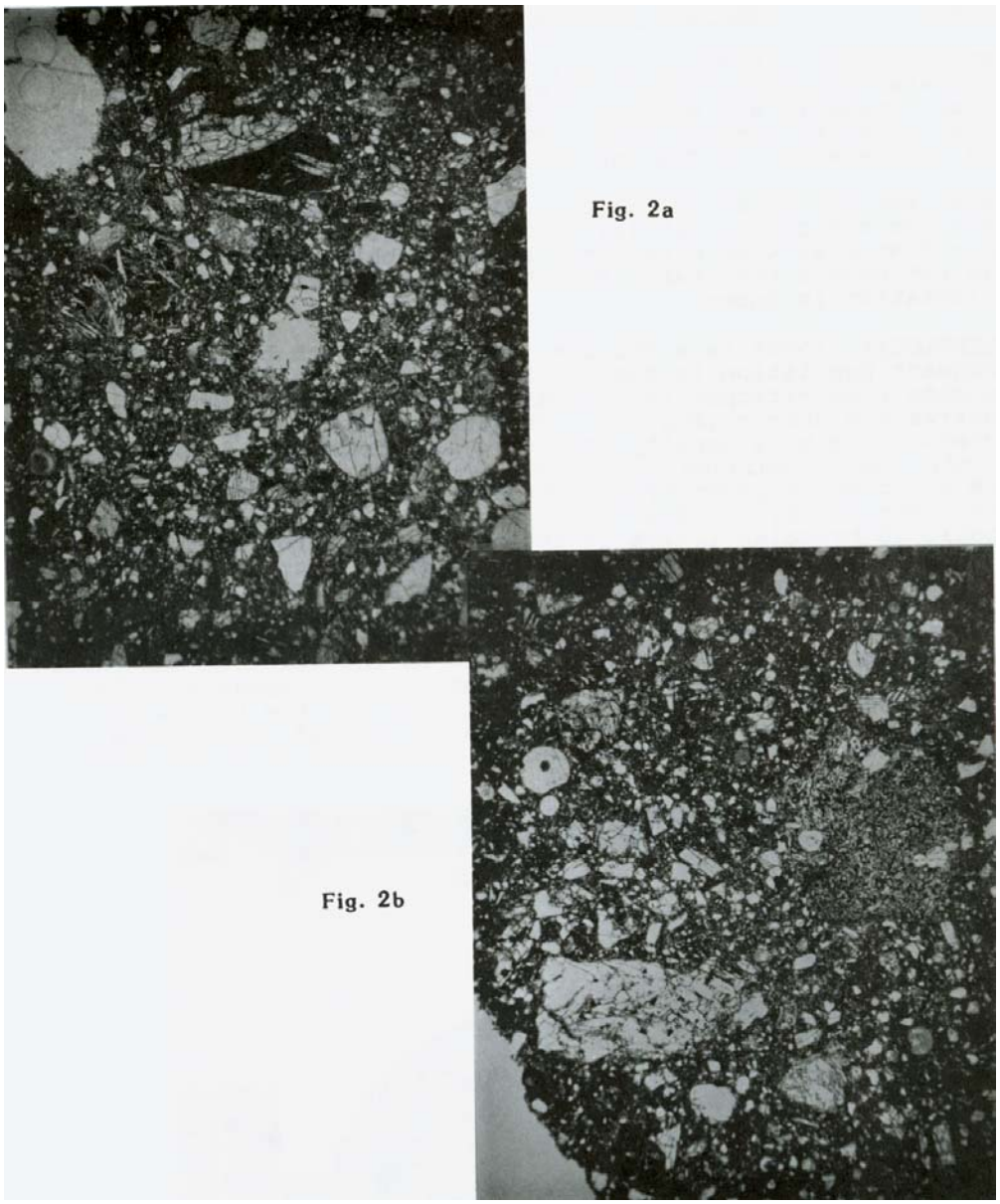

Figure 2. Photomicrographs of 15086,32. Widths about 3mm. Transmitted light,
a) general matrix view, with two vitrophyric quartz-normative
mare basalt clasts in upper right,
b) general matrix view, with coarse mare basalt, lower left,
and a highlands impact melt, middle right.

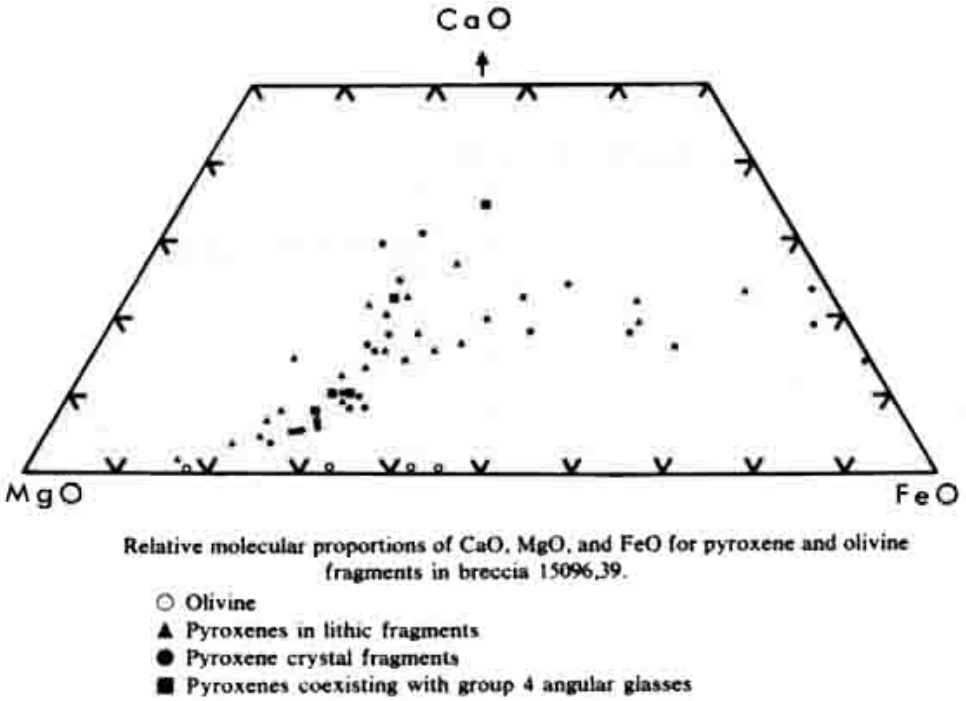

Figure 3. Compositions of pyroxenes and olivines in 15086,39 (Drake and Klein, 1973).

Descriptions of fragmental materials were provided by Drake and Klein (1972, 1973), Brown et al. (1972a), Engelhardt et al. (1972, 1973), and Wenk et al. (1972). The most detailed description is that of Drake and Klein (1972, 1973). They found a diverse range of lithic and glass types and textures, and analyzed 291 glasses, 58 pyroxenes, 27 feldspars, 4 olivines, and 12 lithic clasts (the latter with defocussed beam), providing representative analyses. The lithic clasts include pyroxene porphyries (microporphyritic to vitrophyric), microgabbros, subophitic basalts, and anorthositic gabbros. The "recrystallized" fragments as depicted in Drake and Klein (1973, their Fig. 1d) are actually typical, rapidly crystallized KREEP basalts (Drake and Klein concluded that most lithic clasts were of igneous derivation. This is true, but a few, such as one depicted here in Figure 2b, are highland impact melt breccias, and some are anorthositic granulites). Pyroxenes exhibit diverse chemical compositions (Fig. 3) but individual grains are little zoned; the mineral fragments represent the same population as the lithic population. Only one grain of pyroxferroite was found. Olivines range from $Fo_{91.2}$ to $Fo_{54.6}$, plagioclase from An_{92} to An_{77}. Drake and Klein (1973) distinguished six clusters of glass compositions (Fig. 4). The spheres and some fragments form a cluster corresponding to the well-known Apollo 15 green glass group; other groups are aluminous (24.6 to 28.8% $A1_2O_3$), roughly highland basalt; KREEP (0.3 to 0.9% K_2O); medium-Ti mare (3.8% TiO_2); anorthositic (35% $A1_2O_3$); and a group of brown, opaque glasses with 19% FeO and less than 1% MgO which is similar to the glass of Apollo 15 pyroxene-vitrophyres and may well merely be such material. Brown et al. (1972) also concluded that the sample contained much quartz-normative mare basalt and green glass;

they also observed yellow KREEP and high-Ti (10.4% TiO_2) glass. They found mineral fragments indicative of highlands derivation (An_{97}, $En_{83}Wo_2$, pleonaste, etc.), and found one olivine at Fo_{93} with less than 0.01% CaO; they suggested that this fragment was meteoritic, but it is similar to the olivines in the (lunar) spinel troctolite in 15445.

Wenk et al. (1972) studied plagioclases, loose crystals oriented in thin sections. Most showed only albite twins. They fit the optic curves for terrestrial feldspars, and the probe data suggests the low temperature curve is appropriate. The feldspars clearly are nonstoichiometric, being deficient in Al in comparison with Ca. L. Taylor et al. (1975) found that the compositions of Fe-Ni grains were scattered (Fig. 5) and some fell in the "meteoritic" field, indicating a non-equilibrium assemblage, as expected of a breccia. The opaque mineral population lacks chromite (Fig. 6) indicating that there is not an appreciable contribution from typical coarse-grained gabbros.

L. Taylor et al. (1975) included 15086 in their study of basalt cooling rates as determined from the partitioning of Zr between ilmenite and ulvospinel. The empirical data give a wide scatter, a result of mixing several rock types, and demonstrates that any post-breccia formation reheating and cooling was not of sufficient magnitude to completely equilibrate Zr among the oxides. The average partitioning indicates sources cooled at an average of 16°C/day. Onorato et al. (1979) continued the work of L. Taylor et al. (1975) with a more refined solute partitioning model, using the same data to deduce 5.6° to 9.5°C/day. They found grain-size effect to be negligible for this rock. They gave no indication that this rock is a breccia, and treated it as a basalt.

Uhlmann et al. (1981) used a bulk composition of 15086 (source unstated, but it appears to be microprobe-derived) in experiments to determine glass-forming characteristics and possible thermal histories. From experiments they constructed TTT and CT curves. For their composition (Table 15086-2) they determined a liquidus temperature of 1217°C and a glass transition temperature (Tg) of 677°C. They estimated viscosity-temperature relationships, and tabulated a nucleation barrier of 68KT*. From their simplified model they calculated a cooling rate of 4.5°C/sec necessary to produce a glass, close to their measured rate of 3°C/sec. Uhlmann et al. (1981) erroneously described 15086 as a crystalline matrix breccia; the uncertainty in their bulk composition and the fact that sample is a friable breccia makes the direct application of their results to a thermal history of 15086 inappropriate.

Adams and McCord (1972) plotted the 1 micron and 2 micron pyroxene bands in diffuse reflection spectra against each other. 15086 is fairly intermediate in pyroxene type, at the transition from mare (calcic pyroxene) and non-mare (low-Ca pyroxene), and like 15555.

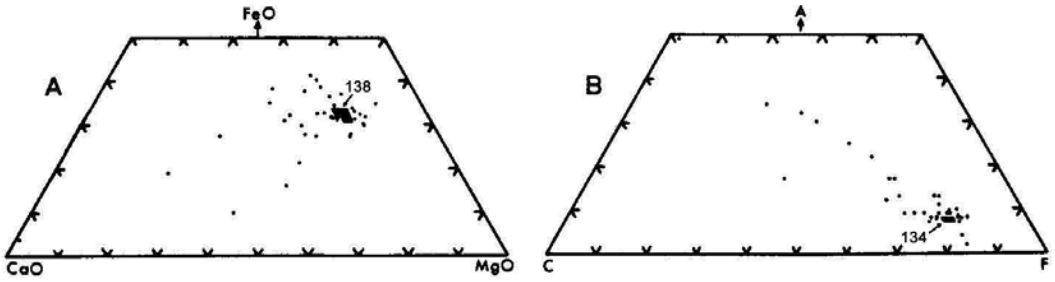

Compositional ranges of rounded glasses in microbreccia, 15086,39. The numbers refer to the total number of analyses plotting in the opaque areas. (a) Relative molecular proportions of CaO, MgO, and FeO. (b) ACF diagram ($A = Al_2O_3 - Na_2O - K_2O$, $C = CaO$, $F = FeO + MgO + MnO$).

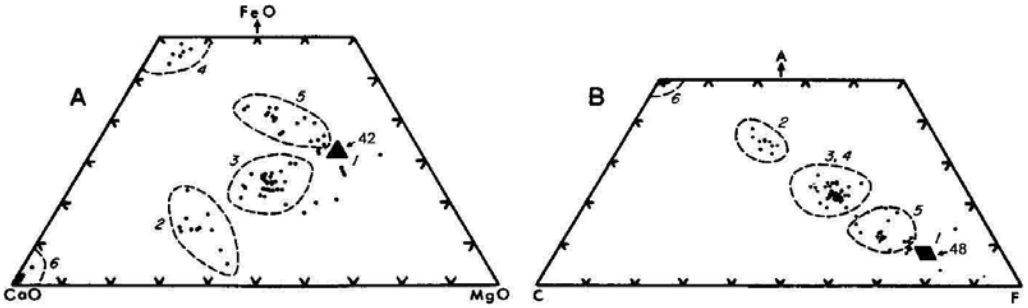

Compositional ranges of angular glasses and irregular patches of glass in microbreccia 15086,39. Numbers refer to sub-group designations described in text. (a) Relative molecular proportions of CaO, MgO, and FeO. (b) ACF diagram ($A = Al_2O_3 - Na_2O - K_2O$, $C = CaO$, $F = FeO + MgO + MnO$).

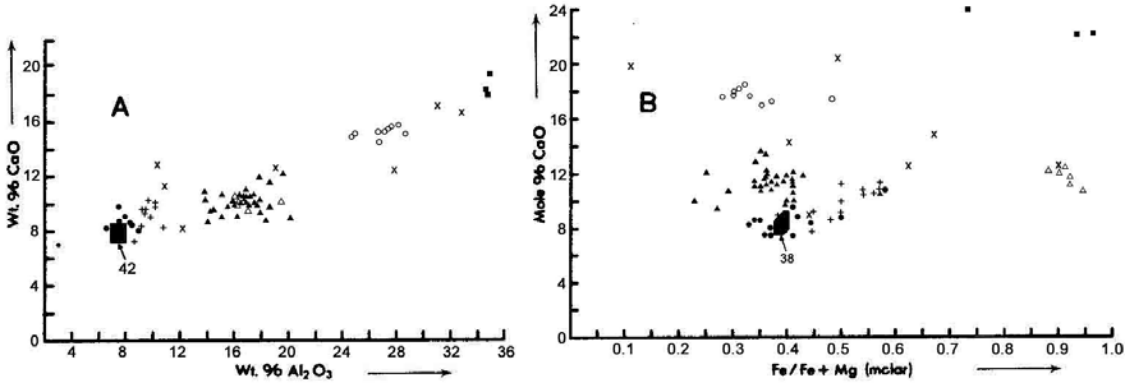

(a) Weight percent CaO vs. weight percent Al_2O_3 in angular glasses. (b) Molecular percentage of CaO vs. atomic fraction of Fe/Fe + Mg.

● Group 1 △ Group 4
○ Group 2 + Group 5
▲ Group 3 ■ Group 6
× Unclassified analyses.

Figure 4. Compositions of glasses in 15086,39 on various plots (Drake and Klein, 1973).

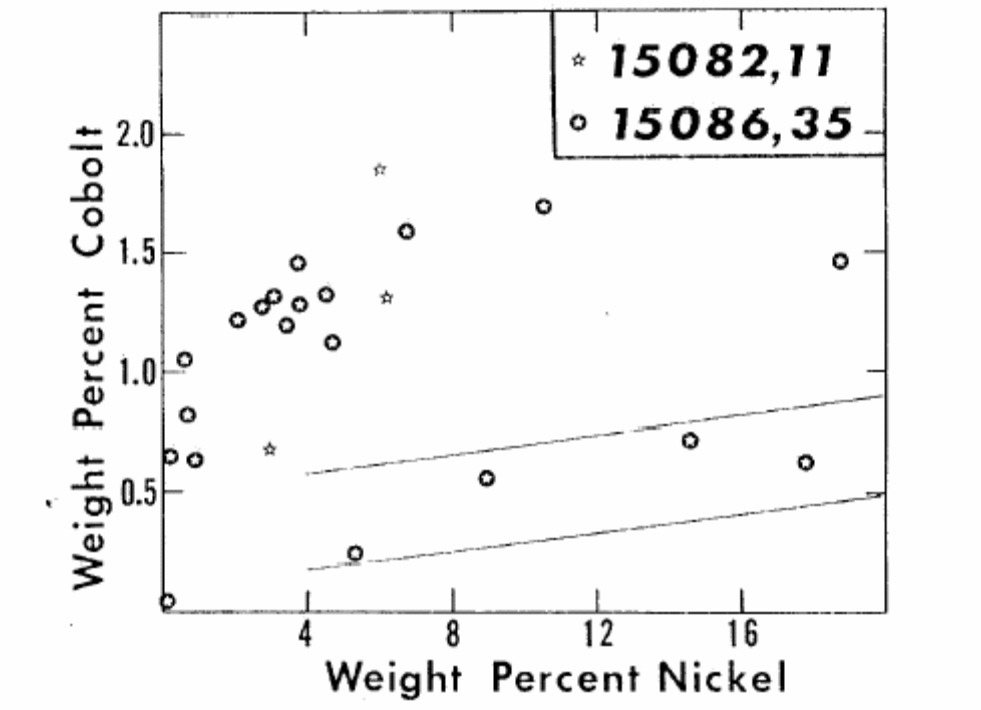

Figure 5. Compositions of metals in 15086, and 15082
(L. Taylor et al., 1976).

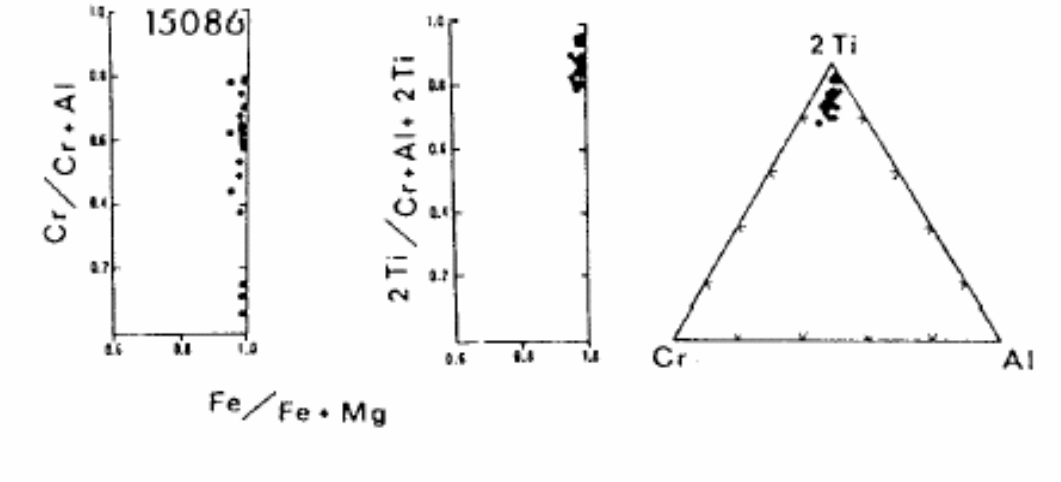

Figure 6. Compositions of spinels in 15086
(L. Taylor et al., 1976).

CHEMISTRY: Bulk rock chemical analyses are listed in Tables 1 and 2, and rare earths are plotted in Figure 7. The analyses in Table 1 show some small differences but generally show 15086 to be quite similar to the local regolith at Station 1. Rose et al. (1975) analyzed for, and found no, Fe_2O_3, and reported an "excess reducing capacity" of +0.63. Thiemens and Clayton (1979, 1980) reported stepwise heating release of nitrogen (Table 3, Fig. 8).

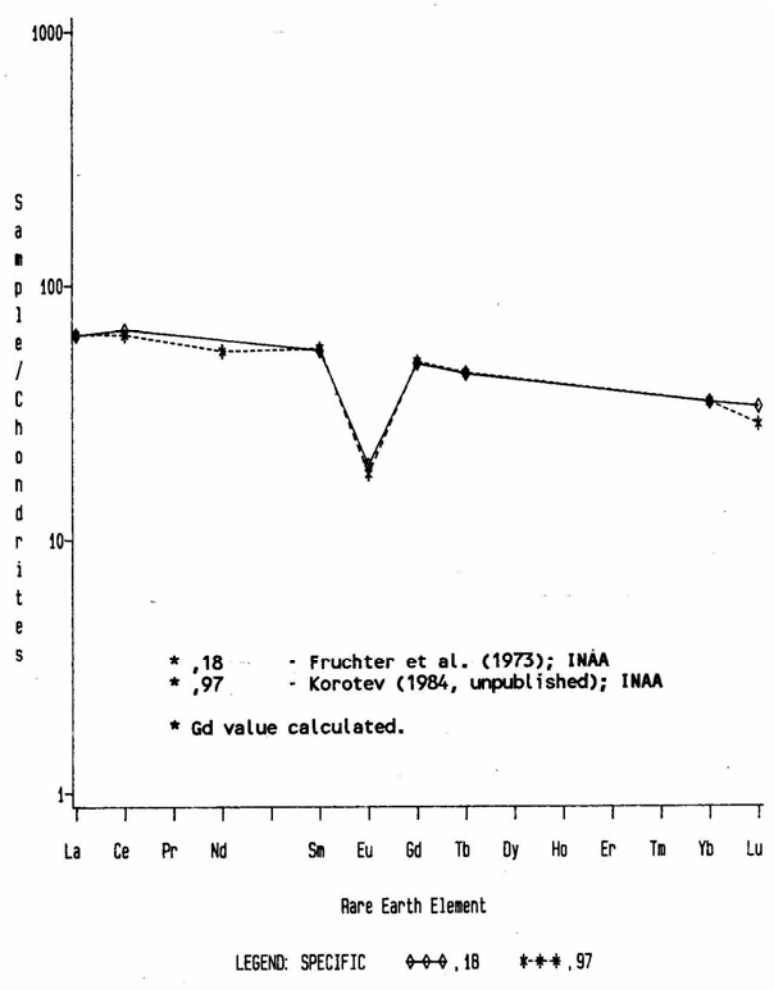

Figure 7. Rare earth elements in bulk samples of 15086.

STABLE ISOTOPES: The nitrogen isotopic data of Thiemens and Clayton (1979, 1980) (Table 3, Fig. 8) shows a pattern very much like that of the ALSEP core section 15003, from a depth of 157 to 146 cm, and is flanked by the 15005 (79 to 82 cm) and 15002 (202 to 205 cm) sections. This feature suggests that 15086 was derived from a similar depth. Cosmogenic ^{15}N is 2.8 ng/g, which also corresponds with a depth of 140 cm in the core, so both implanted and cosmogenic nitrogen suggest a similar depth of origin. The soils had a two-stage irradiation producing a correlation of implanted nitrogen abundance and isotopic composition. 15086 lies close to this line, suggesting a similar two-stage irradiation.

TABLE 15086-1. Bulk rock chemical analyses

		,18	,29	,0	,97	,24	
Wt %	SiO2		47.50				
	TiO2	1.72	1.67				
	Al2O3	12.3	11.01				
	FeO	15.9	17.49		16.0		
	MgO		10.55				
	CaO		10.26		10.0		
	Na2O	0.398	0.35		0.39		
	K2O		0.14	0.172			
	P2O5		0.17				
(ppm)	Sc	33	33		32.1		
	V		92				
	Cr	2700	2876		3010		
	Mn		2015				
	Co	41	42		44.8		
	Ni		79		146		
	Rb		4.1				
	Sr		83		145		
	Y		68				
	Zr	260	234		340		
	Nb		19				
	Hf	7.4			8.2		
	Ba	230	146		214		
	Th	3.7		3.2	3.1		
	U			0.76	1.00		
	Pb		14				
	La	21.0	19		21.1		
	Ce	59			56		
	Pr						
	Nd				33		
	Sm	10.0			10.2		
	Eu	1.35			1.25		
	Gd						
	Tb	2.1			2.11		
	Dy						
	Ho						
	Er						
	Tm						
	Yb	6.9	9.4		6.9		
	Lu	1.13			0.96		
	Li		13				
	Be		2.2				
	B						
	C					57	
	N						36.1
	S						
	F						
	Cl						
	Br						
	Cu		12				
	Zn		28				
(ppb)	I						
	At						
	Ga		5100				
	Ge						
	As						
	Se						
	Mo						
	Tc						
	Ru						
	Rh						
	Pd						
	Ag						
	Cd						
	In						
	Sn						
	Sb						
	Te						
	Cs				220		
	Ta	1400			1040		
	W						
	Re						
	Os						
	Ir				3.0		
	Pt						
	Au				<3		
	Hg						
	Tl						
	Bi						
		(1)	(2)	(3)	(4)	(5)	(6)

References and methods:

(1) Fruchter et al. (1973); INAA
(2) Rose et al. (1975); semi-microchemical, XRF, optical emiss. spec.
(3) Keith et al. (1972); gamma-ray spec.
(4) Korotev (1984 unpublished); INAA
(5) Moore et al. (1973); combustion, gas chromatography
(6) Thiemens and Clayton (1979, 1980); vacuum pyrolysis

TABLE 15086-2. Bulk chemical composition of 15086
(Uhlmann et al., 1981). Method unstated but appears to be microprobe.

Wt %	SiO2	48.3
	TiO2	1.7
	Al2O3	9.6
	FeO	16.9
	MgO	10.0
	CaO	10.0
	Na2O	0.4
	K2O	0.1
ppm	Cr	~2000
	Mn	~2300

RADIOGENIC ISOTOPES AND GEOCHRONOLOGY: Huneke et al. (1974) measured Ar in stepwise heating of clear and devitrified glass spheres handpicked from 15086. Trajectory variations on diagrams to separate ^{40}Ar into trapped and radiogenic contributions are complex. A ^{40}Ar-^{39}Ar age of 3.29 ± 0.06 b.y. for undevitrified green glass from the 1075°C and 1195°C points was determined (Fig. 9); this fraction has 45% of the ^{39}Ar release and very little trapped Ar. Inclusion of the subsequent 1320°C release changes the calculated age only 0.02 b.y. This determination is consistent with and confirms the previous determination of 3.38 ± 0.06 b.y. of Huneke et al. (1973). For devitrified spheres, the last 65% of ^{39}Ar release yields an average apparent age of 3.1 b.y., only slightly younger than the undevitrified samples.

RARE GASES, COSMOGENIC NUCLIDES, TRACKS, MICROCRATERS AND EXPOSURE: Huneke et al. (1974) reported Ar data for stepwise heating release of clear and devitrified green glass spheres. Tbe isotope variations are complex (Fig. 10), and no constant trapped argon composition is clearly established. The data serve to illustrate the complexity in trapped argon compositions. The systematics are better defined in the undevitrified glasses than in the devitrified material.

Hintenberger et al. (1975) provided some He, Ne, Ar, Kr, and Xe isotopic data for a bulk 15086 sample. The ^{132}Xe/^{36}Ar is higher in 15086 and other Apollo 15 breccias than it is in soils, for unknown reasons (these authors erroneously refer in the text and figure caption to Apollo 17 breccias rather than Apollo 15 breccias).

Cosmogenic radionuclide data (Keith et al., 1972) definitely show that ^{26}Al is unsaturated (Keith et al., 1972; Yokoyama et al., 1974) and that 15086 has been exposed to radiation for only 200,000 to 500,000 years. Thiemens and Clayton reported a nitrogen spallation age of 736 m.y.

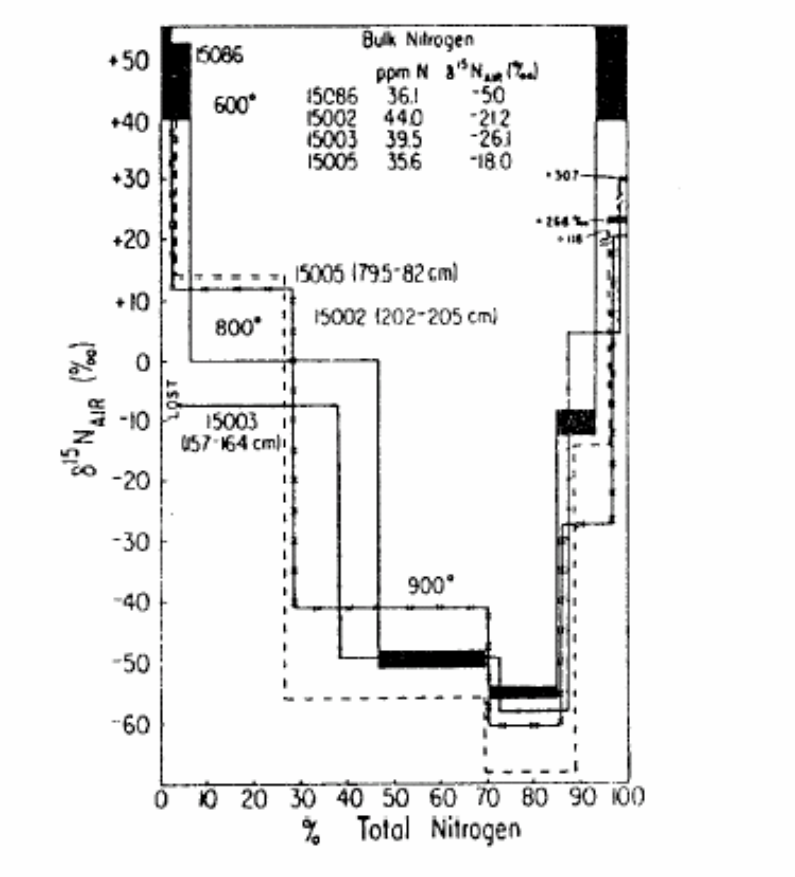

Figure 8. Stepwise heating analysis of 15086 and core samples 15002, 15003, and 15005 (Thiemens and Clayton, 1980).

TABLE 15086-3. Stepwise heating release nitrogen and nitrogen-isotopic data (Thiemens and Clayton, 1980)

Temp °C	N_2 ppm	$\delta^{15}N$ (°/oo)
600	2.4	+46.0
800	14.3	-0.2
900	7.9	-50.0
1000	5.3	-54.6
1100	3.6	-11.0
1300	2.6	+167.5
TOTAL	36.1	-5.0

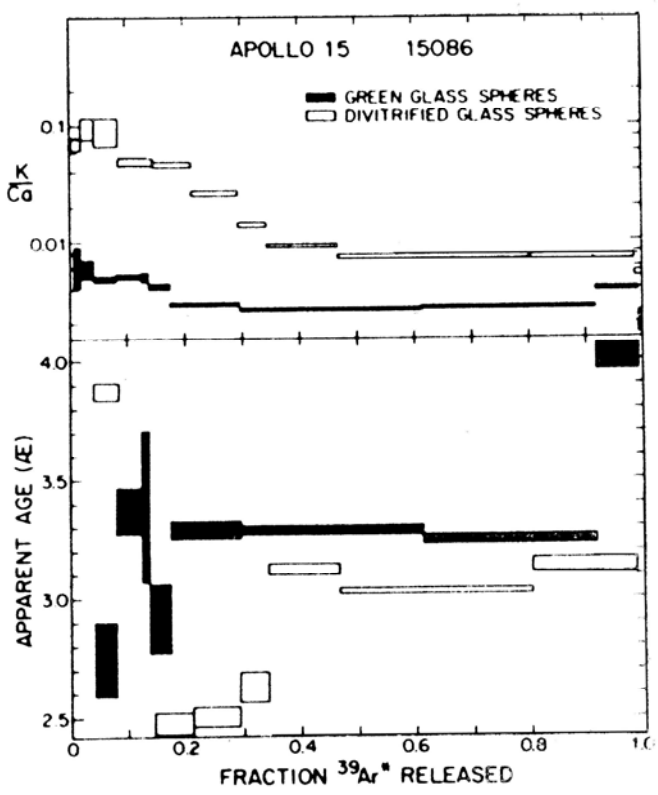

Figure 9. K/Ca and apparent age for green glass spheres and devitrified glass spheres handpicked from 15086 (Huneke et al., 1974).

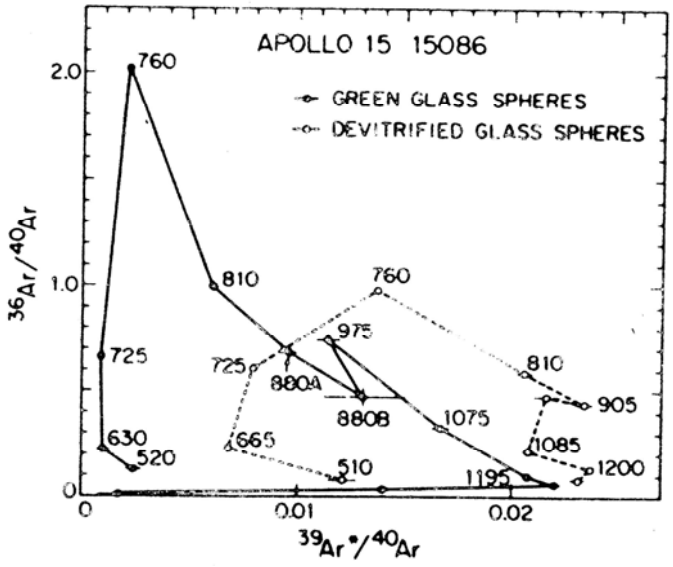

Figure 10. $^{36}Ar/^{40}Ar$ vs. $^{39}Ar^*/^{40}Ar$ for 15086 green glass spheres and devitrified glass spheres handpicked from 15086 (Huneke et al., 1974).

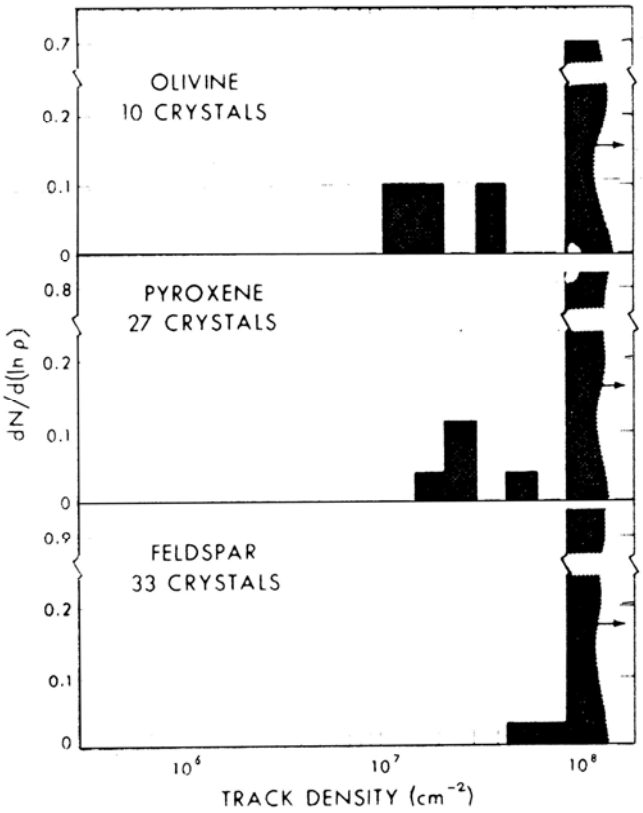

Figure 11. Track density distribution in hand-picked grains from 15086 (Macdougall et al., 1973).

Macdougall et al. (1973) found preserved etchable tracks in glasses, olivines, and feldspars. They showed SEM photomicrographs, including a feldspar with a density gradient. Track density distributions, for grains 50 micron to 300 microns, are shown in Figure 11. The fraction of grains with a density greater than $10^8/cm^2$ (N_H/N) is high, about 0.9. The densities in all three phases are about the same, and the values are typical of soils with a surface exposure of 80 to 100 m.y. (see also Price et al., 1975, for tabulations). The preservation of the tracks in glass indicates that reheating was to no more than 300°C. The green glasses show large and small etch pits, i.e., two distinct track sizes. The large-pit density does not correlate with U, but in a general way with solar flare track density; hence they are not fission tracks but solar tracks from nuclei with Z greater than 26. Even if all the large pits were fission tracks, the "age" would only be 0.7 b.y., raising the question of why the samples lack fission tracks. Macdougall et al. (1973) suggested that the glasses formed more recently than 0.7 b.y. ago, and that the 3.3 to 3.4 b.y. Ar-Ar ages are from some previous event; they cite the slow diffusion of Ar even at 1660°C, above the melting temperature (however, there is a distinct possibility that the calculations of Macdougall et al., 1973, use a much higher U content for the interior of green glass spheres than is actually the case). Goswami et al. (1976) noted that

the track densities greater than $10^8/cm^2$ are consistent with exposure within the upper 1 mm of regolith.

Rajan et al. (1974) studied craters on green glass spheres, and found the micrometeoroid complex to be similar to the contemporary one, with crater morphologies similar to currently produced ones. There is an order-of-magnitude agreement with the present-day flux. Goswami et al. (1976) depicted two SEM photographs of microcraters. Three out of four feldspars and three out of five spherules studied had numerous microcraters with diameters 0.1 to 2 microns. Crater frequency/size for two feldspars are similar to the Murchison meteorite and a variety of uneroded lunar samples, and the craters are a production population. The relationship of craters and tracks gives a production rate for craters larger than 0.5 microns of 3 and 30 craters/cm^2/yr II sr for the two feldspars (assumes 0.5 m.y. age). The differences are possibly a result of shielding. Neither shows a steep profile, so the fluxes are lower limits.

PHYSICAL PROPERTIES: Collinson et al. (1972, 1973) reported natural remanent magnetism (NRM) and rock magnetic data . 15086 has a higher NRM (about 9×10^{-6} emu/g) than mare basalts and is stable after removal of the soft components up to 100 Oe (Figs. 12, 13). There is some evidence for anomalous variations during AF demagnetization. 15086 also has a strong viscous remanent magnetism (VRM), acquiring a field of 130×10^{-6} emu/g in one week (1.0 to 2.0 0e fields), with a corresponding viscosity coefficient of 33.5×10^{-6} emu/g/Oe. This VRM is anomalously stable to AF demagnetization fields in excess of 250 Oe. In comparison, basalts have a low VRM. The rock magnetism results showed that the saturation isothermal remanent magnetism level was 21×10^{-3} emu/g, much higher than basalts. The saturation anhysteric remanent magnetization in 0.6 0e in a peak AF of 1200 Oe was 230×10^{-6} emu/g, about 50 times greater than the NRM. Brecher (1975, 1976) listed 15086 in her proposal of textural remanent magnetization as having "a common pattern of NRM directional change in AF and/or thermal demagnetization," based on the Collinson et al. (1972, 1973) data.

Geake et al. (1973) produced luminescence spectra for 15086; plagioclase is the component mainly responsible for the luminescence characteristics.

PROCESSING AND SUBDIVISIONS: Despite its friability, 15086 was originally sawn to produce a slab through its center, with oriented samples and interior and exterior pieces (Fig. 14). The slab (,3) was immediately split to produce ,4 to ,10 and subsequent daughters. ,10 was made into a potted butt and thin sections ,32 to ,38 made from it. Butt end ,2 was also partly subdivided, including the production of potted butt ,26 for thin sections ,39 to ,43. Later ,2 was entirely subdivided to produce an interior shielded portion and surrounding pieces (,53 to ,58). In 1975 ,0 was further sawn to produce butt end pieces of which ,63 (13.8 g) and ,64 (3.4 g) are in remote storage at Brooks. Subsequent chipping on ,0 produced a few more daughters (including potted butt ,200 which produced thin section ,205). ,0 now has a mass of 33.13 g and is the largest individual piece.

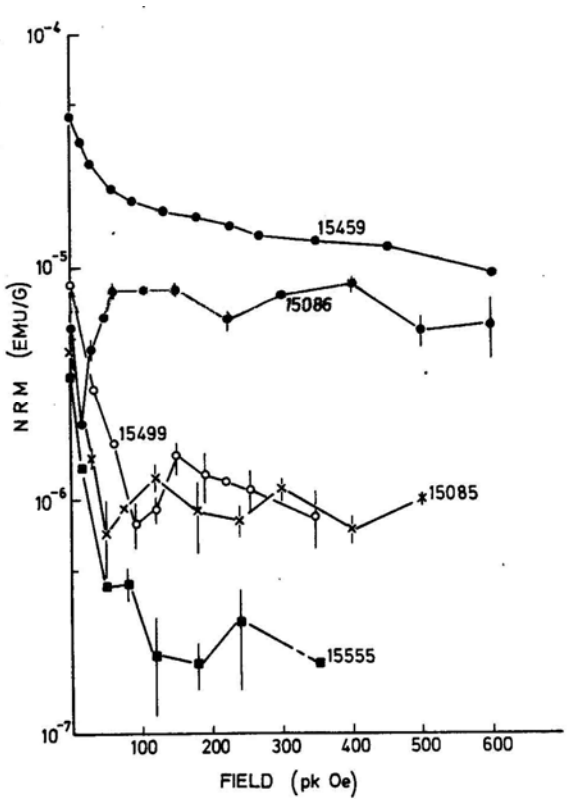

Figure 12. Alternating field demagnetization of Apollo 15 samples including 15086 (Collinson et al., 1973).

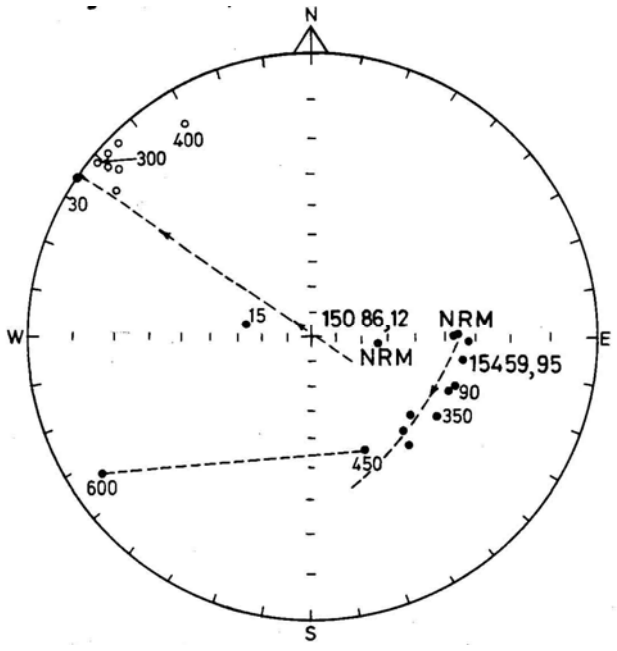

Figure 13. Alternating field demagnetization of 15086 and 15459, referred to arbitrary axes in the rocks (Collinson et al., 1973).

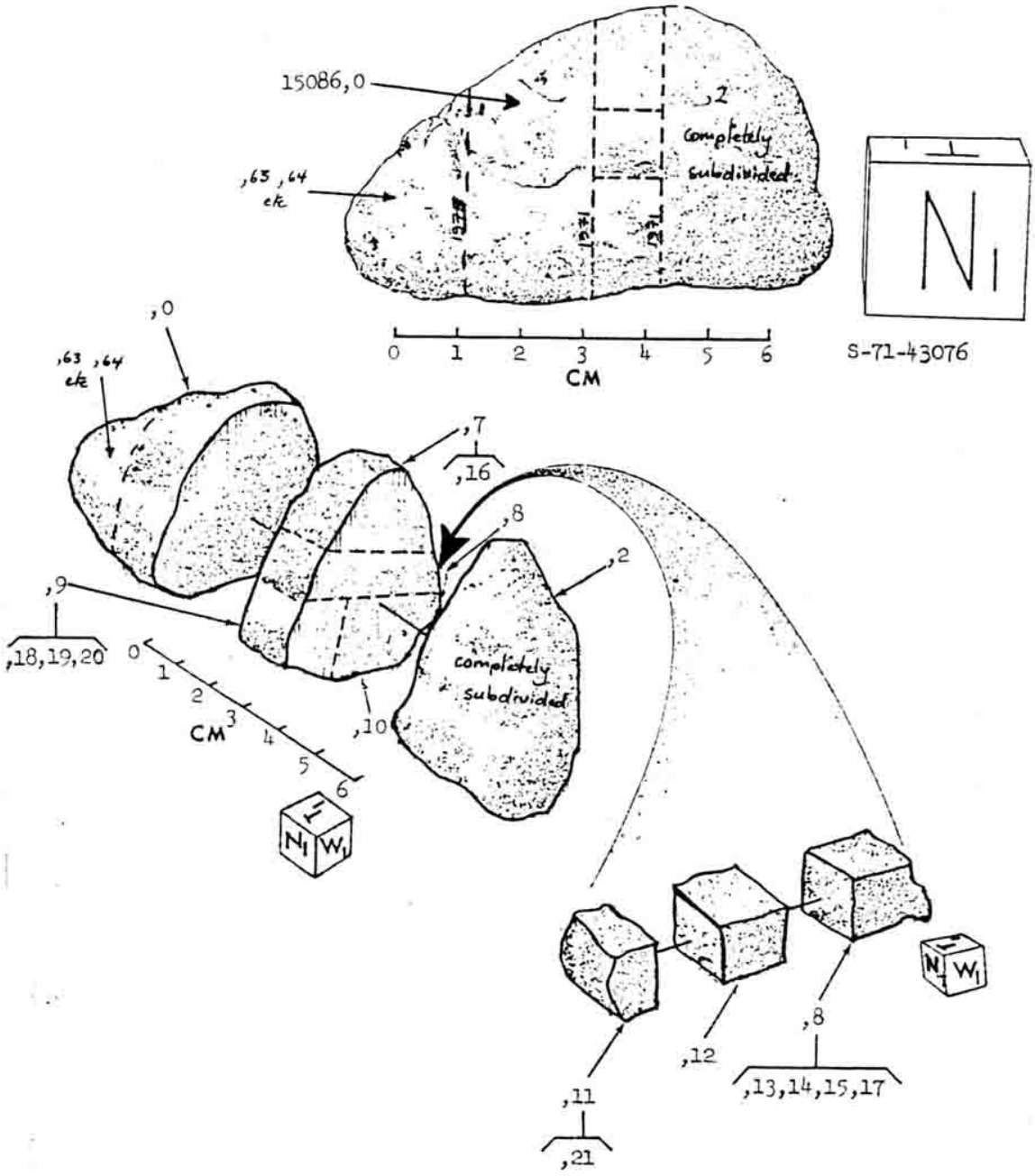

Figure 14. Essential splitting of 15086.